Li *et al. The Journal of Headache and Pain* (2025) 26:115
https://doi.org/10.1186/s10194-025-02059-3

The Journal of Headache and Pain

RESEARCH Open Access

White matter and cortical gray matter microstructural alterations in migraine: a NODDI and DTI analysis

Zhilei Li[1†], Yanliang Mei[2†], Lei Wang[1], Tianhua Fan[1], Cheng Peng[1], Kaibo Zhang[1], Shouyi Wu[1], Tong Chen[3], Zhenchang Zhang[1], Binbin Sui[3*], Yonggang Wang[2,1*] and Xueying Yu[2*]

Abstract

Background The pathophysiological mechanism of migraine remains elusive, thereby impeding the effective treatment of the disease. Current neuroimaging research focuses on changes in brain functional connectivity, functional networks, and macrostructural alterations, which reflect abnormal neuronal function during the disease process. The plasticity changes in neuronal structures and neurotransmitter system dysregulations potentially play a crucial role in migraine onset and chronicity of migraine. This study utilizes multimodal neuroimaging techniques to investigate the microstructural and neurotransmitter alterations in migraine and provides new insights into its pathological mechanisms and therapeutic method.

Methods Microstructural alterations in both white matter (WM) and cortical gray matter (GM) were evaluated among 40 chronic migraine (CM) patients, 35 episodic migraine (EM) patients, and 45 healthy controls (HCs) using Diffusion Tensor Imaging (DTI) and Neurite Orientation Dispersion and Density Imaging (NODDI) models. Tract-based spatial statistics (TBSS) and Surface-based analysis (SBA) were performed to compare groupwise differences in white and gray matter microstructure, respectively. Furthermore, the cross-modal toolbox JuSpace was used to analyze the correlation between cortical gray matter neurite alterations and neurotransmitter.

Results In the WM, compared to HC, a decrease in neurite density index (NDI) was identified in the migraine group, and both NDI and fractional anisotropy (FA) were decreased in the CM group. No significant alterations were observed in the EM group. An increase in radial diffusivity (RD) was found in the CM group compared to the EM group. In the cortical GM, compared to HC, the migraine group had fewer neurites in the right insula and temporal pole cortex, and the CM group showed a reduction in neurites in the right middle temporal and fusiform cortex. The cortical GM

†Zhilei Li and Yanliang Mei contributed equally to this work.

*Correspondence:
Binbin Sui
reneesui@163.com
Yonggang Wang
w100yg@gmail.com
Xueying Yu
yuxueying6@aliyun.com

Full list of author information is available at the end of the article

of neurite damage was negatively correlated with neurotransmitters in migraine and CM. There was no correlation between NODDI and DTI metrics of these brain regions and clinical data after the Bonferroni correction.

Conclusion Our findings indicated that neurite loss was detected in both WM and cortical GM of migraineurs. As the migraine progresses into chronicity, the axonal damage may become more pronounced. The neurite damage of cortical GM was negatively related to neurotransmitters.

Keywords Migraine, Neurite orientation dispersion and density imaging, Diffusion tensor imaging, Tract-based Spatial statistics, Surface-based analysis, Microstructure

Background

Migraine is a common neurological disorder with an enormous burden for individuals and socioeconomic systems [1]. The global prevalence of migraine is estimated to be 14 ~ 15%, with a prevalence of 8.6% in men and 17.0% in women. Migraine can be classified into episodic migraine (EM) and chronic migraine (CM) according to the frequency, duration, and accompanying symptoms of the headache. The EM progresses to the CM at a rate of 2.5 ~ 3.0% per year, while the CM affects approximately 1 ~ 2% of the global population. Migraine is prone to affect individuals in the prime of their lives and is related to several comorbidities, significantly compromising patients' quality of life [1–5]. However, pathophysiological mechanisms and progression of migraine and its subtypes remain unclear.

As neuroimaging technologies develop, the migraine pathogenesis theories shift from peripheral vascular theory to those centered on central neural mechanisms. The research of functional magnetic resonance image (fMRI) has confirmed the significant neuronal activity in relevant brain regions of migraine [6]. The existing research has demonstrated the remodeling of neuronal structure in chronic pain conditions [7]. The Golgi staining of migraine animal model with nitroglycerin and cortical spreading depression (CSD) showed reduced neuronal complexity in associated brain regions, and a CGRP inhibitor reversed neurite growth [8]. Previous studies of structural and diffusion MRI have shown altered brain macroscopic structure (e.g. local gray matter volume, cortical thickness, surface area, gyrus index and white matter fiber bundles integrity) in patients with migraine [9, 10]. These findings provided indirect evidence of transformations in neural tissue plasticity and adaptation. Recent studies have attempted to employ the advanced diffusion magnetic resonance imaging (dMRI) technique NODDI (Neurite Orientation Dispersion and Density Imaging) to investigate microstructural alterations in white matter among migraine patients. A small sample NODDI study of white matter found decreased orientation dispersion index (ODI) in the medication overuse migraine group, with no statistical difference among other subgroups [11]. A Mendelian randomization study found that decreased ODI in the right posterior thalamic radiation was associated with an increased risk of migraine [12]. The above research utilized the NODDI model to conduct a preliminary investigation of the white matter of migraine-affected brains, establishing methodological foundations for microstructural investigations in migraine. However, they adopted a monomodal analytical approach and did not consider the microstructural alterations of cortical gray matter. Therefore, we applied a traditional diffusion tensor imaging (DTI) model combined with the NODDI model, a biophysically grounded framework quantifying neurite morphology through orientation dispersion and density metrics, to perform a multiscale assessment of the brain microstructure in both white and gray matter among migraine patients [13].

In addition, multiple neurotransmitters, including opioids, glutamate, GABA, and dopamine, play active roles in the cortical modulation of the nociceptive processing [14]. Current research indicates that migraine is closely associated with neurotransmitter systems, including serotonergic [15], dopaminergic [16], GABAergic, and glutamatergic systems [17], all of which are critically involved in the pathophysiological mechanisms of migraine. Neurotransmitters, as chemical messengers that transmit signals among neurons, neurons, and effector cells, may play a pivotal role in the onset and chronication of migraine. However, the relationship between neurotransmitter and microstructural remodeling of cortical neurons of migraine remains to be elucidated. The JuSpace is a software package for integrating various imaging modalities and neurophysiological measures derived from positron emission tomography (PET) [18]. This toolbox was utilized to investigate relationships between neurotransmitters and neuronal plasticity in migraine.

Our research hypothesizes that migraine is associated with (1) reduced neurite density in both white matter and cortical gray matter, reflecting microstructural degradation. (2) These microstructural changes are expected to manifest as reduced neurite density, with both white matter and cortical gray matter damage potentially being more pronounced in CM compared to EM. (3) These microstructural alterations in white matter tracts and cortical areas may contribute to the underlying

mechanisms of migraine onset and chronication. (4) Alterations in the microstructure of cortical gray matter may be associated with neurotransmitters.

Materials and methods

Study design and ethics

The design of this study was cross-sectional, and the research was conducted as a case-control study. The study was based on the China Headache Disorders Registry Study (CHAIRS; ClinicalTrials.gov Identifier: NCT05334927). The research was granted ethical approval by the Ethics Committee of Beijing Tiantan Hospital, Capital Medical University (number: KY2022-044). The entire study was conducted in strict adherence to the principles of the Helsinki Declaration (1975) and the National Statement on Ethical Conduct in Research Involving Human Subjects (1999). It is declared that no conflicts of interest are held by the authors of this study.

Study subjects

Participants who met the criteria were divided into three groups including HC ($n = 45$), EM ($n = 35$), and CM ($n = 40$). All the participants were enrolled in the HeadacheCenter, Department of Neurology, Beijing Tiantan Hospital, CapitalMedical University from October 2020 to October 2023. Demographic data, body mass index (BMI), headache duration, Visual Analogue Scale (VAS), Patient Health Questionnaire-9 (PHQ-9), Headache Impact Test-6 (HIT-6), Generalized Anxiety Disorder-7 (GAD-7), Migraine Disability Assessment (MIDAS), and Pittsburgh Sleep Quality Index (PSQI) were recorded for all participants. All the patients with migraine had no history of aura and medication overuse. All patients were scanned during the interictal period. The interictal period was defined as ≥ 72 h from the preceding and following attacks [19]. A mild headache was reported in 1 EM and 2 CM participants during scanning. The criteria for inclusion of migraineurs: (1) All the migraineurs were diagnosed according to ICHD-3 [5]; (2) The age range is from 16 to 65 years; (3) No contraindications to MRI examination (e.g. claustrophobia, metal in the body); (4) All patients demonstrated right-hand dominance; (5) A complete set of imaging data and clinical information was available for all patients. Criteria for exclusion of patients with migraine: (1) Other types of primary headaches; (2) Secondary headache; (3) Inaccurate diagnosis; (4) Other conditions that can lead to overuse of analgesics, such as musculoskeletal disorders and rheumatic diseases; (5) The poor quality of the imaging data (significant susceptibility artifact or incomplete raw MRI data); (6) The incompleteness of the clinical information; (7) Notable brain lesions or white matter hyperintensities (Fazekas score above 1, especially around the lateral ventricular body). The inclusion criteria for HCs were: (1) Fulfilment of MRI scan requirements (no claustrophobia syndrome, no metals in the body, etc.); (2) Absence of neurological or other major systemic diseases; (3) Match with age, gender of migraineurs. Exclusion criteria: (1) Pregnancy or lactation; (2) Contraindication to MRI; (3) Poor quality MRI data (significant susceptibility artifact or incomplete raw MRI data); (4) Obvious brain lesions or white matter hyperintensities, with Fazekas score exceeding 1, particularly at the level of the lateral ventricular body.

MRI data acquisition

MRI images were obtained using a 48-channel Signa Premier 3.0T superconducting magnetic resonance imaging scanner. T1-weighted images were acquired using MP-RAGE sequences. The specific parameters are as follows: sagittal acquisition, field of view (FOV) = 250×250 mm^2, slice number = 192, flip angle = 8°, preparation time = 880 ms, recovery time = 400 ms, acceleration factor = 2, acquisition time = 4 min, and $1 \times 1 \times 1$mm^3 of spatial resolution. A multi-shell spin-echo echo-planar imaging sequence was employed to capture diffusion-weighted images based on the specified parameters: repetition time = 5285 ms, echo time = 85 ms, data matrix = 104×104, field of view = 208×208 mm^2, slice thickness = 2 mm, slices = 78, gradient direction = 108, and diffusion sensitivity coefficients (b) = 0, 1000, and 2000s/mm^2, 50 diffusion-weighted directions at each b-value and 9 b0 scans. During the MRI procedure, participants were required to remain awake and relaxed and to keep their eyes closed. To minimize noise and head motion during scanning, earplugs and cushioning foam pads were made available.

MRI data preprocessing

Before pre-processing, two experienced neuroradiologists visually examined each participant's diffusion and T1-weighted images for significant artifacts. Briefly, the preprocessing procedure included rectification of eddy current artifacts, reduction of noises, rectification of inter-volume head motion artifacts, and extraction of brain tissue. Images were processed by using the FMRIB software library (FSL, version 6.0.1; http://www.fmrib.ox.ac.uk/fsl). The *dcm2niigui* tool was used to convert the DICOM format of all diffused data into NIFTI format. The *topup* tool was applied for estimating and correcting susceptibility induced distortions by using anterior to posterior encoding direction and posterior to anterior phase-encoding direction. We used the *eddy_openmp* command to correct head motion and eddy current distortions. Brain masks from the b0 image of each participant was created by using FSL's *BET* (Brain Extraction Tool).

DTI model and metric computation

DTI is a simple data-driven model. It is widely used to study white matter in the brain. Key indicators of the DTI model include fractional anisotropy (FA), mean diffusivity (MD), axial diffusivity (AD), and radial diffusivity (RD). Quantitative assessment of global white matter alterations can be achieved through computational summation of diffusion tensor-derived fiber vectors [20]. It makes DTI more sensitive to white matter. FMRIB's Diffusion Toolbox (FSL-FDT, http://fsl.fmrib.ox.ac.uk/fsl/fslwiki/FDT) was used to correct for motion, eddy current correction and gradient directions. The pre-processed image data was analyzed using the FSL toolbox *DTIFIT*, based on a diffusion tensor model, to calculate the FA, MD, AD, and RD values.

NODDI model and metric computation

The NODDI is currently one of the most advanced diffusion models. Its feature is the integration of MRI signals with the biological information of neural tissue, increasing the biological interpretability of the results. The principle of the NODDI model is based on the division of each voxel into three compartments: the neurite, the CSF, and the extra-neurite tissue [21]. It makes more definitive tissue pointing. The NODDI model outperforms the traditional DTI model because of its ability to assess neurite density and orientation in WM and GM and minimize the volume effects [22, 23]. This makes it a promising technique for clinical applications [24, 25]. The main metrics of the NODDI model include neurite density index (NDI), orientation dispersion index (ODI), and isotropic volume fraction (ISOVF) [24]. The reliability of the NODDI model has been confirmed in various neurological and psychiatric disorders, including through post-mortem studies and animal models [26, 27]. The NODDI MATLAB toolbox (version 1.0.5; https://www.nitrc.org/projects/noddi_toolbox) was used with default p arameters to produce maps of NDI, ODI and ISOVF. The usual biological interpretation of the NODDI metric is that a decrease in NDI indicates neurite loss, a decrease in ODI suggests a reduction in neurite complexity, and an increase in ISOVF indicates inflammation [28, 29].

Cortical reconstruction based on freesurfer

T1 structural images were reconstructed using FreeSurfer version 6.0 (https://surfer.nmr.mgh.harvard.edu). The tasks of image processing included head motion correction, removal of non-brain tissue, segmentation of brain tissue, cortical reconstruction, and cortical surface inflation.

Tract-based Spatial statistical analysis (TBSS)

Compared to traditional voxel-based method, TBSS merges the advantage of voxel and fiber tract analysis, resolves issues aligning and smoothing nuclei, and enhances sensitivity, objectivity, and interpretability in results [30]. The *DTIFIT* toolbox within FSL was employed to generate the FA, MD, AD and RD maps based on the DTI model. The FA map threshold was set at 0.2, and the average FA was calculated for all subjects. FA images were thinned to generate an average FA skeleton. The MD, AD, RD, NDI, ODI and ISOVF skeletons were generated by the "*tbss_non_FA*" script. The white matter skeleton is composed of voxels located in the core of the white matter, avoiding contamination by voxels signaling from adjacent tissues. To validate the robustness of our results, intergroup comparisons of total intracranial volume (TICV) were systematically performed. The results indicated no statistically significant intergroup differences in TICV (all $p > 0.05$; Table S1-2). In this investigation, the non-parametric white matter skeleton was calculated using FSL randomization command, with adjustments made for sex and age as covariates. A corrected P-value was obtained by performing threshold-free cluster enhancement (TFCE) and 5000 permutations. Statistical significance for the white matter voxels was determined at a corrected P-value<0.05 following adjustment for multiple comparisons using the family-wise error (FWE) rate control.

Surface-based analysis (SBA)

The SBA had significant advantages over traditional voxel-based methods. It preserves the spatial continuity of cortical structures and minimizes the contamination of cortical gray matter by the CSF and the white matter [31].The initial step entailed the alignment of the NODDI map with the T1 structural image, utilizing a 6-degrees-of-freedom boundary-based registration (BBR). Subsequently, the mid-thickness surface was built. It minimized interference from signals of surrounding tissues. The NODDI measures (NDI, ODI, ISOVF) for each subject were projected onto the surface at mid-thickness. In the final step of the process, the projected maps were resampled into the template of surface space for the analysis in the future. All surface maps were smoothed using a Gaussian kernel filter with a full width at half maximum (FWHM) of 10 mm. The smoothing procedure was performed on the surface after projecting the relevant metrics from cortical vertices, thereby enhancing the accuracy of the statistics [32–34].

Spatial correlation between cortical Gray matter neurites damage and neurotransmitter maps

The JuSpace toolbox facilitated cross-modal spatial correlations between neuroimaging and the nuclear imaging (https://github.com/juryxy/JuSpace). The JuSpace toolbox explored spatial interactions between neurite damage and receptors/transporters. The average

neurotransmitter map was generated from PET/SPECT of independent healthy volunteers, and processed according to the methods outlined in the JuSpace publication, including rescaling and normalizing of Montreal Neurological Institute space [18]. We aimed to known whether spatial pattern of NDI in patients with migraine, compared to HCs, resembles distribution of nuclear imaging-derived neurotransmitter maps from independent healthy volunteer populations included in the toolbox, such as D1/D2 receptor, dopamine transporter (DAT), 6-fluoro-(18 F)-L-3,4-dihydroxyphenylalanine (FDOPA), 5-HT1b receptor, 5-HT1a receptor, 5-HT2a receptor, serotonin transporter (SERT), noradrenaline transporter (NAT), μ-opioid receptors (MU), kappa opioid receptor (KappaOp), vesicular acetylcholine transporter (VAChT), cannabinoid 1 receptor (CB1), metabotropic glutamate receptor 5 (mGluR5), N-methyl-D-aspartic acid receptor (NMDA) and gamma-aminobutyric-acid type a (GABAa). The toolbox was utilized to extract groups mean values from neurotransmitter and NDI maps, with a particular focus on GM regions from neuro-morphometrics atlas. The mean regional values of patients' NDI maps were extracted and z-transformed with respect to HCs. Spearman correlation coefficients (Fisher's z-transformed) were computed between the z-transformed NDI maps of patients and spatial distribution of neurotransmitter maps. The distribution of observed Fisher's z-transformed individual correlation coefficients was tested for significant deviation from zero by calculating exact permutation-based p-values in the JuSpace, which involved 10,000 orthogonal permutations randomly assigning group labels. Spatial autocorrelation was adjusted by the computing partial correlation coefficients between the NDI and the neurotransmitter, while local GM probabilities, estimated from the SPM12-provided TPM.nii, were used for adjustment. False discovery rate (FDR) correction (Benjamini-Hochberg procedure) was employed for multiple comparison correction, using a P-value threshold of 0.05 [18, 35, 36].

Statistical analysis

The Kruskal-Wallis H test assessed differences from non-normally distributed data, such as age and BMI. Gender differences were analyzed using the Chi-square test. The clinical scales were tested using Independent Samples t-tests or Mann-Whitney U test. FSL Randomize tool (version 2.1), a permutation-based statistical inference method known as "*randomize*," was employed to compare voxel-wise TBSS differences in FA, MD, AD, RD, NDI, ODI, and ISOVF values of white matter across groups, utilizing TFCE. For the reliable statistical results, 5000 iterations were carried out. Finally, the significance threshold was set at $p < 0.05$ after correction for multiple comparisons (two-sided, FWE correction). To analyze differences in cortical NODDI metrics between migraine subgroups and healthy controls, we applied the mri_glmfit tool to fit a generalized linear model (GLM). All the results from the Monte Carlo simulations (uncorrected $p < 0.01$) were corrected for multiple comparisons (using mri_glmfit-sim function) with 10,000 iterations, for both hemispheres, and the clustering threshold was $p < 0.05$. In the statistics, age and gender were incorporated as covariates, and the statistics were adjusted for multiple comparisons. The positive results were visualized on the inflated surfaces of the brain cortex. Correlations between the DTI and NODDI metrics and clinical characteristics (duration of migraine, VAS scores, HIT-6 scores, PHQ-9 scores, GAD-7 scores, PSQI scores, MIDAS scores, and MoCA scores) were assessed through Pearson's correlation analysis. The Bonferroni correction method was conducted for the significance test, with threshold set at $p < 0.05/N$ (where N represents the number of correlation analyses performed).

Results

Demographic data and neuropsychological evaluations

There were 128 participants in this study, including 46 HC, 37 EM, and 45 CM. After conducting quality control, one HC participant was excluded for poor MRI data quality. Five CM participants were excluded, two for poor MRI data quality and three for the significant white matter hyperintensities. Likewise, two EM participants were excluded, one due to poor MRI data quality and the other due to the white matter hyperintensities (Fig. 1). There were no statistically significant differences in age, gender, and BMI among three groups. The CM group showed higher PHQ-9 score, GAD-7 score, PSQI score, and MIDAS score (Table 1).

TBSS analysis based on the DTI and NODDI model

The DTI and NODDI models were employed to provide an objective evaluation of the pathological changes in white matter in both the migraine group and the HC, as well as among the subgroups. To enhance the robustness of the results, only fiber tracts with more than 30 voxels were included in the analysis [37] (Tables 2, 3 and 4). The migraine group demonstrated a reduction of NDI values in fiber bundles such as the right superior longitudinal fasciculus (SLF), inferior longitudinal fasciculus (ILF), inferior frontal-occipital fasciculus (IFOF), cingulum (hippocampus) (CGH), and uncinate fasciculus (UF) compared to HC (Fig. 2). After performing multiple comparison corrections, there was no significant variation existed between the migraine and HC regarding DTI indicators. Next, we compared white matter differences across the migraine subgroups (EM and CM) and HC. Compared to HC, the CM exhibited reduced FA and NDI values (Fig. 3). Fiber bundles with reduced FA values are

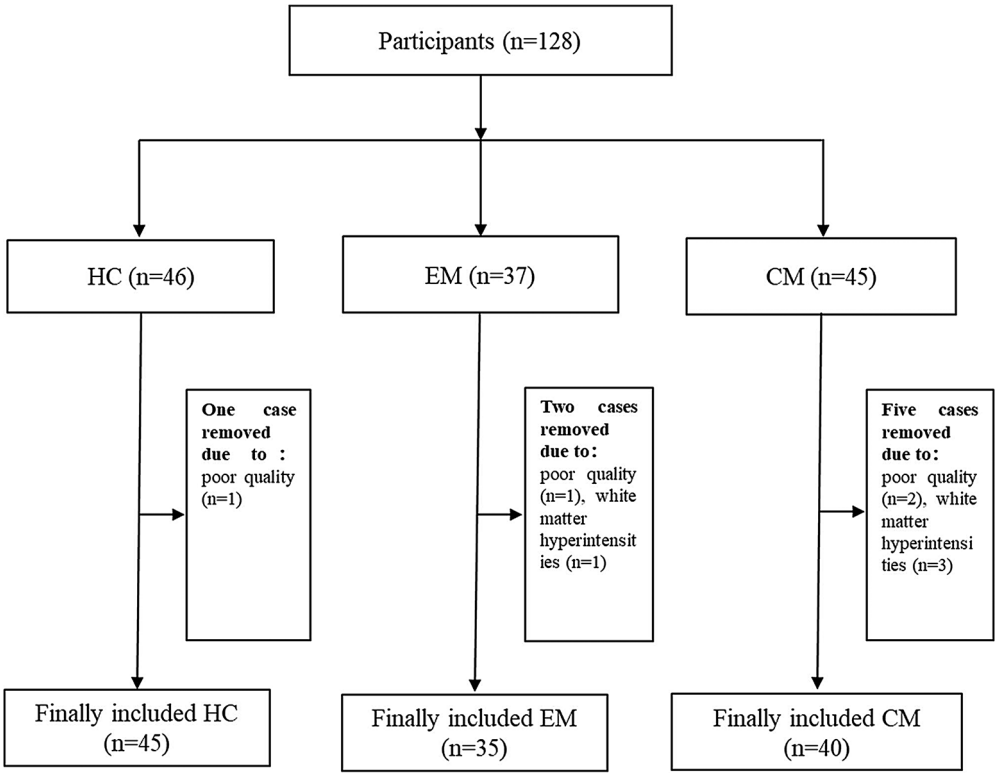

Fig. 1 Participant inclusion-exclusion process flowchart. HC, healthy control; EM, episodic migraine; CM chronic migraine

Table 1 Clinical and demographic features of participants

	Controls (*n* = 45)	EM (*n* = 35)	CM (*n* = 40)	*P*-value
Ages (years)	35(19)	37(20)	39.50(30.50)	0.843[a]
BMI (kg/m^2)	23.15(4.15)	22.23(4.60)	23.95(3.53)	0.207[a]
Gender (female/male)	27/18	23/12	29/11	0.479[b]
Headache history (years)	NA	11(16)	11(18.25)	0.463[c]
Pain intensity VAS score	NA	7(2)	7(2.75)	0.314[c]
HIT-6 score	NA	65.23 ± 7.53	66.05 ± 6.76	0.62[d]
PHQ-9 score	NA	4(7)	9(8.75)	<0.001[c]
GAD-7 score	NA	3(5)	6(8.5)	0.024[c]
PSQI score	NA	8.03 ± 4.59	10.73 ± 5.29	0.022[d]
MoCA score	NA	28(3)	28(4)	0.957[c]
MIDAS score	NA	48(46)	83.5(119.25)	0.001[c]

Note: NA, not applicable; BMI, body mass index; VAS, Visual Analogue Scale; PHQ-9, Patient Health Questionnaire-9; GAD-7, Generalized Anxiety Disorder-7; PSQI, Pittsburgh Sleep Quality Index; HIT-6, Headache Impact Test-6; MoCA, Montreal Cognitive Assessment; MIDAS, Migraine Disability Assessment Scale

Data are presented as mean ± standard deviation or as median [interquartile range, IQR]

[a] Kruskal-Wallis H test

[b] Chi-square test

[c] Mann–Whitney U test

[d] Independent Samples t test

all right of SLF, ILF, IFOF, CGH, UF, cingulum (cingulate gyrus) (CG) and anterior thalamic radiation (ATR). Fiber tracts with reduced NDI values are all right of SLF, ILF and UF. Additionally, RD was significantly elevated in CM compared to EM (Fig. 4). Fiber tracts with increased RD values are bilateral SLF, right ILF, right IFOF, bilateral ATR, right body of corpus callosum (BCC) and left corticospinal tract (CST). White matter changes did not show significant differences between the EM and HCs.

SBA analysis based on NODDI model

In the current study, we compared differences in neurites within the gray matter of the cortex between HCs and migraine group (including EM and CM). The migraine group showed fewer neurites in the right insula and temporal pole cortex when compared to HC (Fig. 5; Table 5). Patients with CM showed a reduction in neurites across several brain regions, including the right middle temporal and fusiform cortex, compared to HC (Fig. 6; Table 6). The patients with EM revealed no statistical difference in neurite when compared to HC or patients with CM.

Result of correlation analysis

Correlation analysis using Pearson's method was applied to extracted indicator value in brain regions from Tables 2, 3, 4, 5 and 6 and clinical variables. Regrettably, following Bonferroni correction for the multiple

Table 2 White matter regions of statistically significant differences in NDI between migraine and HCs

Contrast	Cluster	Region	Side	Voxels	*P*-value	MNI coordinate		
						x	y	z
Migraine< HC								
	Cluster1			1477	0.042	49	3	-16
		ILF	R					
		UF	R					
	Cluster2	ILF	R	78	0.049	40	-20	-29
	Cluster3	IFOF	R	257	0.047	32	-22	-23
	Cluster4	ILF	R	530	0.048	34	-36	-21
	Cluster5	ILF	R	116	0.049	44	-46	-20
	Cluster6	ILF	R	47	0.049	44	-35	-20
	Cluster8	CGH	R	222	0.048	20	-41	-8
	Cluster9	SLF	R	37	0.049	55	-34	-9

Note: Inferior longitudinal fasciculus (ILF), Uncinate fasciculus (UF), Inferior frontooccipital fasciculus (IFOF), Cingulum (hippocampus) (CGH), Superior longitudinal fasciculus (SLF); HC, Healthy control; NDI, Neurite density index; R, right. Regions with clusters greater than 30 voxels were contained in this table

Table 3 White matter regions of statistically significant differences in FA and NDI between CM and HCs

Metric	Contrast	Cluster	Region	Side	Voxels	*P*-value	MNI coordinate		
							x	y	z
FA	CM< HC								
		Cluster1	CGH	R	192	0.047	30	4	-34
		Cluster2			830	0.045	43	-18	-19
			ILF	R					
			IFOF	R					
		Cluster3	ILF	R	468	0.041	53	-1	-8
		Cluster4	CG	R	3082	0.048	16	-28	30
		Cluster5			1227	0.041	36	37	0
			IFOF	R					
			UF	R					
		Cluster6	SLF	R	1227	0.040	33	-4	-41
		Cluster7	SLF	R	302	0.043	43	-41	20
		Cluster9	SLF	R	47	0.048	33	-46	20
		Cluster10	SLF	R	192	0.043	52	-23	29
		Cluster11	SLF	R	50	0.044	38	-23	37
		Cluster13	ATR	R	32	0.049	21	25	35
NDI	CM< HC								
		Cluster1	ILF	R	412	0.049	41	4	-34
		Cluster2	SLF	R	924	0.048	53	-31	-20
		Cluster4	ILF	R	59	0.050	46	-13	-23
		Cluster5	SLF	R	99	0.049	53	-11	-23
		Cluster6			426	0.048	49	3	-15
			ILF	R					
			UF	R					
		Cluster7			40	0.050	50	-26	-14
			ILF	R					
			SLF	R					
		Cluster8			69	0.048	49	-34	-12
			SLF	R					
			ILF	R					

Note: Cingulum (hippocampus) (CGH), Inferior longitudinal fasciculus (ILF), Inferior frontooccipital fasciculus (IFOF), Cingulum (cingulate gyrus) (CG), Uncinate fasciculus (UF), Superior longitudinal fasciculus (SLF), Anterior thalamic radiation (ATR); CM, Chronic migraine; HC, Healthy control; FA, fractional anisotropy; NDI, Neurite density index; R, right. Regions with clusters greater than 30 voxels were contained in this table

Table 4 White matter regions of statistically significant differences in RD between CM and EM

Metric	Contrast	Cluster	Region	Side	Voxels	*P*-value	MNI coordinate		
							x	y	z
RD	CM> EM								
		Cluster1			1347	0.044	42	-34	-8
			ILF	R					
			IFOF	R					
		Cluster2	ILF	R	117	0.048	54	-11	-23
		Cluster3			227	0.048	35	-56	-9
			IFOF	R					
			ILF	R					
		Cluster4	ATR	R	59	0.049	29	-26	-6
		Cluster5	IFOF	R	63	0.049	32	-27	3
		Cluster6	ILF	R	45	0.049	54	-26	7
		Cluster8			580	0.043	33	-40	33
			ILF	R					
			SLF	R					
		Cluster10	SLF	L	557	0.048	-38	-7	40
		Cluster12	BCC	R	478	0.048	17	2	35
		Cluster13			1066	0.044	-20	-20	48
			CST	L					
			ATR	L					
		Cluster14	SLF	R	432	0.048	30	-15	43
		Cluster17	SLF	R	127	0.045	-26	-8	43

Note: Inferior longitudinal fasciculus (ILF), Inferior frontooccipital fasciculus (IFOF), Anterior thalamic radiation (ATR), Superior longitudinal fasciculus (SLF), Body of corpus callosum (BCC), Corticospinal tract (CST); CM, Chronic migraine; EM, episodic migraine; HC, Healthy control; RD, Radial diffusivity; L, left; R, right. Regions with clusters greater than 30 voxels were contained in this table

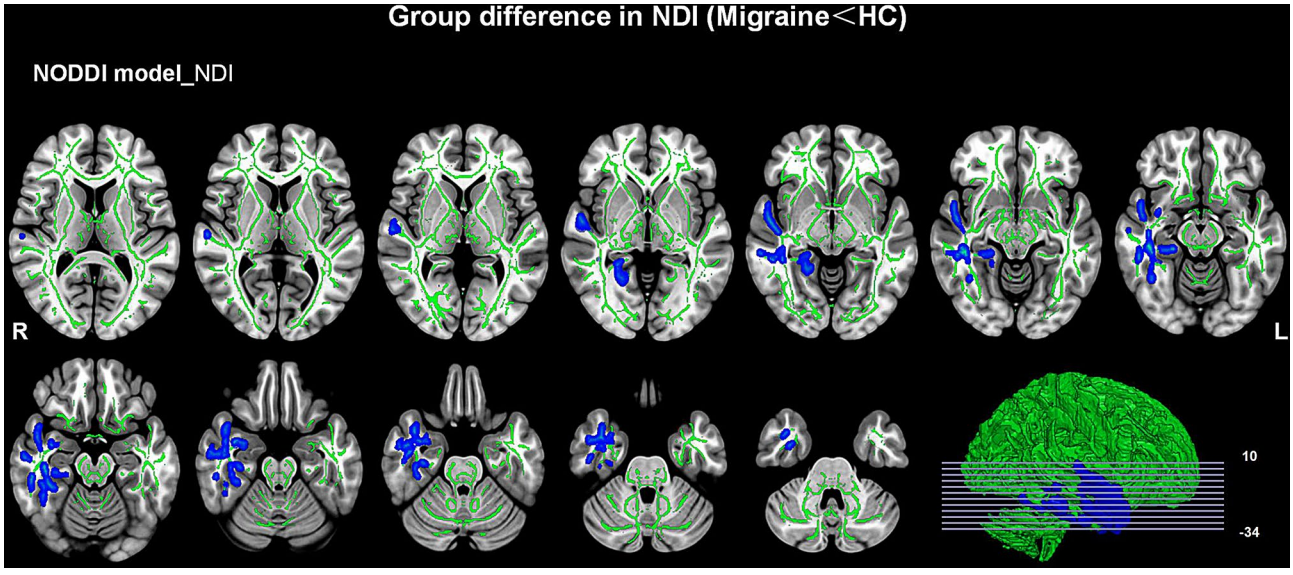

Fig. 2 White matter regions (blue) showed decreased NDI in patients with Migraine compared to HCs group (P_{FWE} < 0.05). HC, healthy control; NDI, neurite density index; L, left; R, right

comparisons, no statistically significant relationships were detected between the regional NDI, FA, and RD values and the clinical characteristics ($p > 0.05$). Compared to HC group, the migraine group was correlated with the four neurotransmitter profiles, namely SERT (r = -0.117, $p = 0.019$ FDR corrected), D2 (r = -0.120, $p = 0.011$ FDR corrected), DAT (r = -0.116, $p = 0.029$ FDR corrected) and FDOPA (r = -0.102, $p = 0.024$ FDR corrected) (Fig. 7A). The spatial distribution of the D2 (r = -0.106, $p = 0.039$ FDR corrected) was related to CM (Fig. 7B). The negative correlation coefficients for both groups indicate neurite

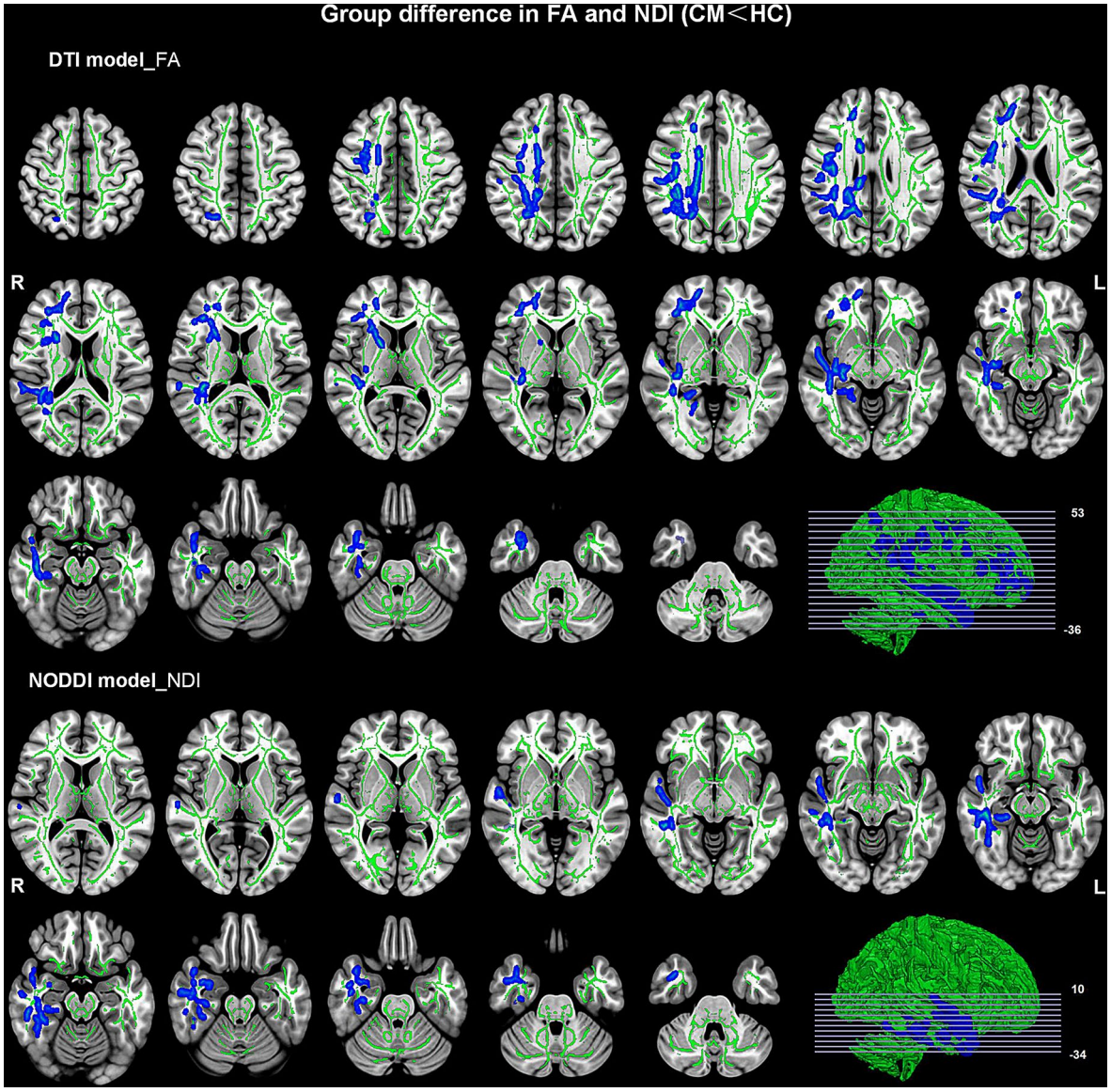

Fig. 3 White matter regions (blue) showed decreased FA and NDI in patients with chronic migraine compared to HCs group ($P_{FWE} < 0.05$). CM, chronic migraine; HC, healthy control; FA, fractional anisotropy; NDI, neurite density index L, left; R, right

reduction in patients compared to HC in areas with high neurotransmitter density.

Discussion

Here, we investigated microstructural alterations in white matter and cortical gray matter among migraine and its subtypes, using NODDI and DTI models combined with TBSS and SBA. Compared to the HC group, the migraine and CM group showed reduced axons in several fiber bundles. Meanwhile, the demyelination was significant in the CM group compared to the EM group. Compared to the HC group, migraine group exhibited reduced dendrite in the right insula and right temporal pole cortex, while the CM group showed reduced dendrite in the right middle temporal gyrus and right fusiform cortex. Furthermore, multimodal spatial correlation analysis revealed that the spatial pattern of cortical neurite damage in migraine group negatively correlated with the spatial distribution of SERT, D2, DAT, and FDOPA. The spatial distribution of D2 was negatively correlated with the spatial pattern of neurite damage in the CM group (Fig. 8). Our observed findings support the hypothesis of neuronal remodeling and neurotransmitter alterations in migraine and its subtypes. It provides preliminary evidence for the pathological mechanisms involving impaired brain microstructure and neurotransmitter imbalance following repeated nociception stimuli.

The microstructural integrity of white matter and cortical gray matter is pivotal in sensory processing and pain modulation, providing a medium for communication

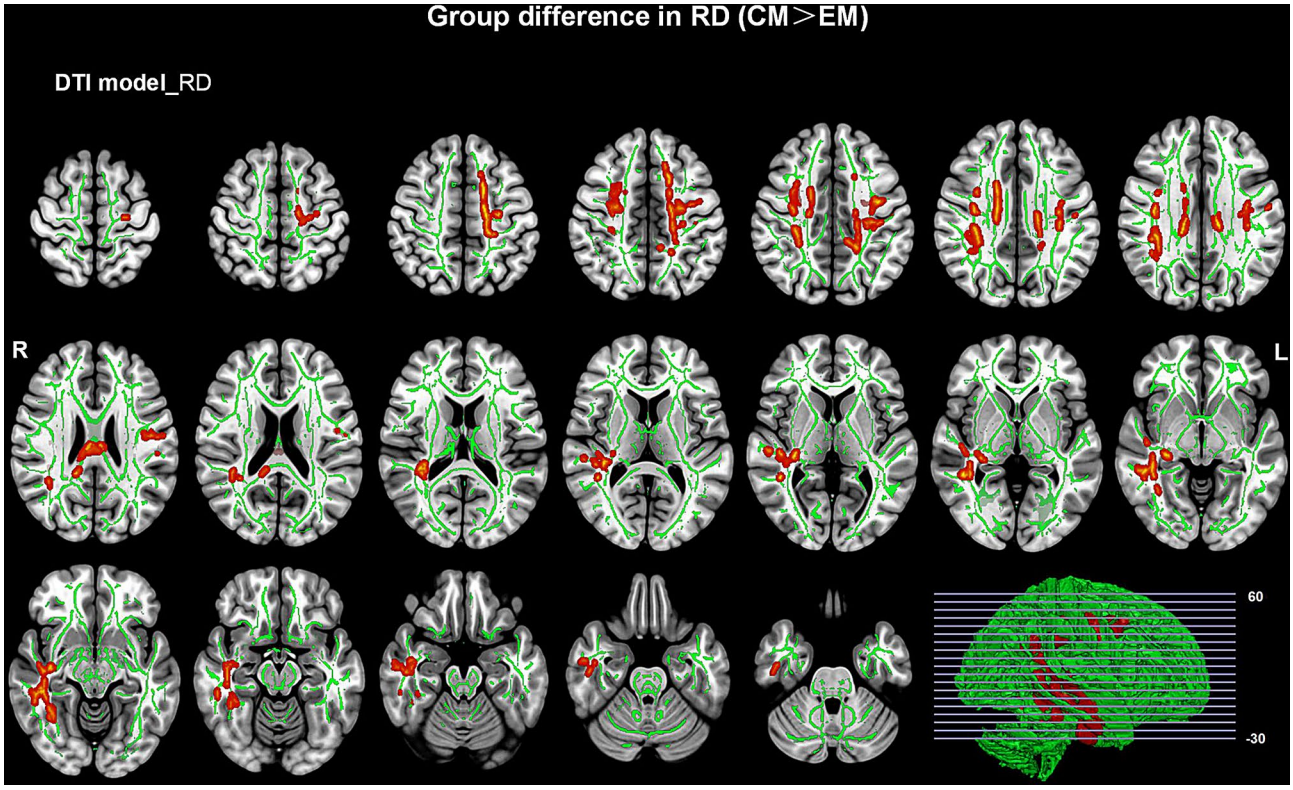

Fig. 4 White matter regions (red yellow) showed increased RD in patients with CM compared to EM group (PFWE < 0.05). CM, chronic migraine; EM, episodic migraine; NDI, neurite density index L, left; R, right

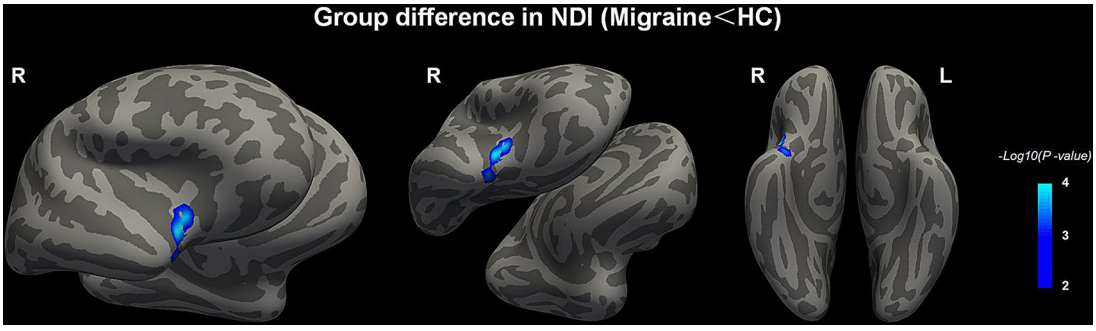

Fig. 5 Gray matter regions (blue) showed decreased NDI in the Migraine group compared to HCs group. HC, healthy control; NDI, neurite density index; L, left; R, right

Table 5 Brain region with NDI changes in migraine

Brain region	Side	MNI coordinates			Cluster sizes (mm^2)	CWP
		x	y	z		
Insula and Temporal pole cortex	R	39.9	-1.1	-19.9	365.07	0.044

Note: The Desikan-Killiany atlas was used to localize brain regions. MNI, Montreal Neurological Institute; NDI, Neurite density index; R, right. CWP, Cluster-wise corrected p-value, $p < 0.05$

between brain regions implicated in pain perception. Previous studies employing DTI models to detect WM alterations in migraine and its subgroups have predominantly emphasized global WM changes, yet lack tissue specificity, and inconsistent are findings reported across investigations [10, 38]. Macroscopic neuroimaging studies have identified cortical thickness and surface area of alterations in related brain regions of migraine [39, 40]. It has been not clear what type of changes in neural tissue leads to the remodeling of cortex. We first applied DTI and NODDI models to identify the specific tissues involved in the pathological damage of white

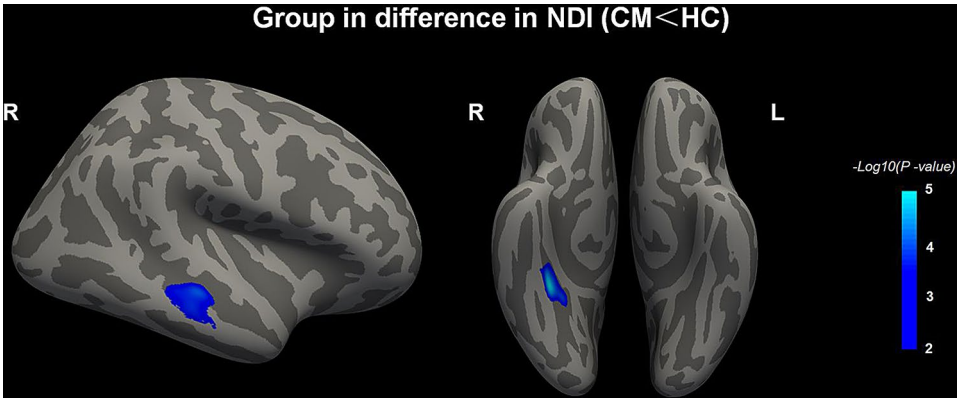

Fig. 6 Gray matter regions (blue) showed decreased NDI in the chronic migraine group compared to HCs group. CM, chronic migraine; HC, healthy control; NDI, neurite density index; L, left; R, right

Table 6 Brain region with NDI changes in CM

Brain region	Side	MNI coordinates			Cluster sizes (mm^2)	CWP
		x	y	z		
Middle temporal	R	46.2	-26.3	-10.1	424.95	0.018
Fusiform	R	35.8	-39.7	-16.9	373.26	0.039

Note: The Desikan-Killiany atlas was used to localize brain regions. CM, chronic migraine; MNI, Montreal Neurological Institute; NDI, Neurite density index; R, right. CWP, Cluster-wise corrected p-value, $p < 0.05$

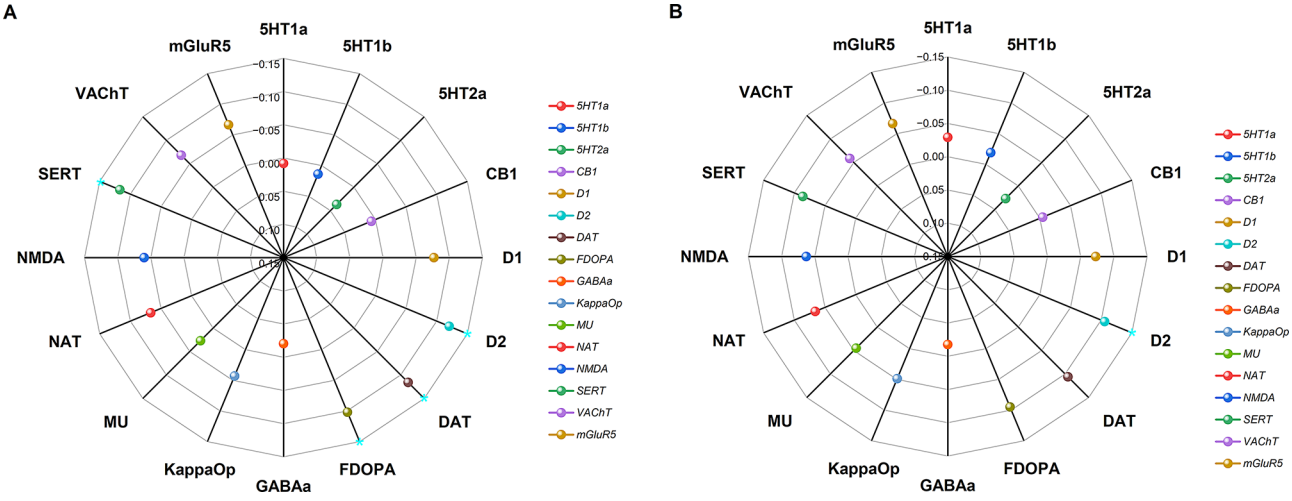

Fig. 7 Spatial correlation between cortical neurites alteration and nuclear imaging-derived neurotransmitter distribution. **A** Reduction of cortical gray matter neurites induced by Migraine vs. HC comparisons was associated with the spatial distribution of serotonin transporter and dopamine D2, dopamine transporter and 6-fluoro-(18 F)-L-3,4-dihydroxyphenylalanine neurotransmitter maps. **B** Reduction of cortical gray matter neurites induced by CM vs. HC comparisons was associated with the spatial distribution of dopamine D2 neurotransmitter maps. *p<0.05 (FDR correction); CM, chronic migraine; HC, healthy control; FDR, false discovery rate; 5HT1a, serotonin 5-hydroxytryptamine receptor 1a; 5HT1b, serotonin 5-hydroxytryptamine receptor 1b; 5HT2a, serotonin 5-hydroxytryptamine receptor 2a; SERT, serotonin transporter; D1, dopamine 1 receptor; D2, dopamine 2 receptor; DAT, dopamine transporter; FDOPA, 6-fluoro-(18 F)-L-3,4-dihydroxyphenylalanine; CB1, cannabinoid 1 receptor; GABAa, gamma-aminobutyricacid type a; KappaOp, Kappa Opioid Receptor; MU, μ-opioid receptor; NAT, noradrenaline transporter; NMDA, N-methyl-D-aspartic acid receptor; VAChT, vesicular acetylcholine transporter; mGluR5, metabotropic glutamate receptor 5

and gray matter in migraine and its subtypes. Compared to HC, the migraine group exhibited reduced NDI values in the NODDI model, while the DTI model showed negative results. Existing research using the DTI technique did not identify significant differences in white matter between migraine and HC [37, 41]. It was not difficult to understand, likely due to the inherent limitations of the DTI model, which was less sensitive to microstructural changes [22]. Furthermore, being involved in different subgroups within migraine group further increased the difficulty of detection. In particular, it should be noted that the differences in acquisition

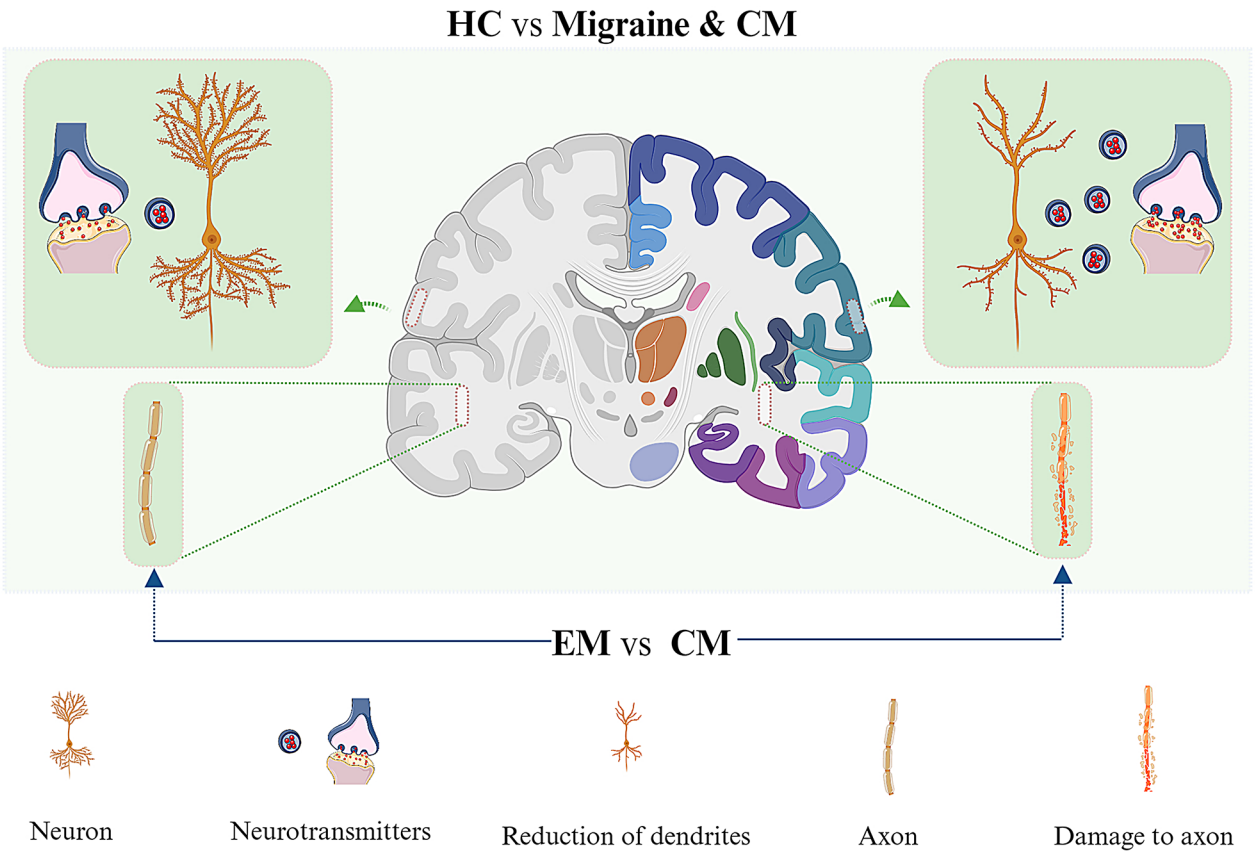

Fig. 8 This is an overview of brain microstructural changes in migraine and its subtypes. Neurite damage is a pathological feature of migraine. With chronicity of migraine, axonal injury or demyelination becomes more severe. Across several brain regions, cortical neurites are diminished in both migraine and CM. The loss of cortical gray matter neurites is negative associated with neurotransmitters. It was created with http://www.biorender.com/. HC, Health control; EM, episodic migraine; CM, chronic migraine

and analysis parameters might also be responsible for influencing the results [42]. However, some DTI studies also reported alterations of WM in migraine [43, 44]. As anticipated, the NODDI model successfully detected neurites loss in patients with migraine. In CM, a reduction in FA and NDI was noted, emphasizing the clear and robust evidence of axonal injury. Meanwhile, reduction of dendrites was observed in the cortical regions of CM. The cortico-subcortical microstructural alterations may reflect potential neuroanatomical substrates contributing to migraine chronification. Compared to EM, higher RD values were observed in the WM fiber tracts of CM. It suggested remarkable demyelination in the white matter of CM. Integrated NODDI and DTI findings demonstrate progressive axonal demyelination and eventual axonal loss with migraine chronification, while cortical gray matter analysis revealed no analogous degenerative changes. There were no statistically significant differences between EM and HC, potentially due to the restrictions of current neuroimaging techniques in detecting subtle changes [45]. In conclusion, our multimodal analysis identified the pathological features of neurites damage in migraine, especially the marked neurites reduction and severe demyelinating changes in CM.

This research identifies that axonal injury of white matter tracts may be involved in the central mechanisms underlying the onset and chronification of migraine. The SLF, ILF, UF and IFOF are the major fiber bundles connecting frontotemporal parieto-occipital regions, which are involved in multiple functions such as visual processing, emotion regulation, and cognitive control [46–48]. These fiber tracts connect multiple brain regions for long-range information transfer and processing. They are susceptible to damage. It had been reported that SLF was impaired in patients with depression and deteriorated with the progression of the condition. SLF incompleteness was observed in migraineurs with comorbid anxiety and depression, highlighting the potential role of SLF in the negative mood dynamics of migraine [10, 49]. This finding is consistent with the higher anxiety and depression scores observed in CM compared to EM. Consistent with findings described herein, Rayan et al. found increased RD rates in ILF associated with pain symptoms in patients with chronic pain, suggesting axonal

damage is associated with pain processing [50]. The UF connected the lateral orbitofrontal and limbic regions which involved in pain, mood, and emotion [51]. Pathological impairment of ILF and UF may correlate with elevated MIDAS scores in patients with CM. The IFOF integrates visual information, and integrity breaking may lead to disorder in visual working memory [48]. It has been known that CSD plays an important role in the pathological mechanism of migraine. The impairment of IFOF connections may interfere with the flow of information from the occipital cortex to the relevant areas of the brain. This damage may lead to increased excitability in the occipital cortex. Increased excitability may be easy to trigger CSD and lead to recurrent migraine attacks [12]. The corpus callosum (CC) connects the two cerebral hemispheres and provides interhemispheric integration and transmission of information [52]. It also played a role in inhibiting pain [53]. Compared to EM, significant demyelinating changes in the BCC of CM patients may contribute to headache chronification. The primary function of the CG is to participate in the processing of pain and emotions [54]. Microstructural changes in the CG of migraineurs might affect headache and emotional processing. The ATR primarily connects the anterior thalamus to the prefrontal cortex and is involved in pain regulation [55]. CHONG et al. also reported extensive demyelinating alterations of ATR in migraine, suggesting its important role in the pathophysiological process of migraine [56]. The CST origin in the primary and secondary motor and somatosensory cortex and extends into the spinal cord. It is a descending fiber tract that is vital for nociceptive perception [57]. The study of fMRI has shown altered functional connectivity between the periaqueductal gray matter and precentral regions in migraineurs [58]. We previously found partial axonal reduction within the CST in a white matter study of the new daily persistent headaches [59]. Compared to EM, the CST demyelination damage was observed in CM. Demyelination of descending pain-modulatory fibers may contribute to the mechanisms underlying migraine chronification.

Reduced neurite density within cortical gray matter in migraine and its subtypes is first evidenced, with significant decreases demonstrated across multiple brain regions. The reduced NDI in the right insula and temporal pole cortex of migraineurs indicated significant changes in the neuroanatomy of these areas. The insula plays a crucial role in interoception, emotional processing, and the integration of sensory information. The VBM- and FreeSurfer-based studies of cortex morphology suggested reduced cortex volume and surface area of insula in migraine [39, 40]. The studies of fMRI and network mapping confirmed the centrality of the insula in migraine [60–63]. The reshaping of dendrites in the insula offers an objective explanation for its macroscopic structural and functional alterations, further underscoring the pivotal role of this region in the pathophysiological mechanisms of migraine. The temporal pole is robust anatomical connectivity with the limbic system, mediating the integration of high-order sensory processing with primary affective responses [64, 65]. The studies of task-state fMRI have demonstrated that the temporal pole is involved in multisensory integration and pain processing through the activation of multiple relevant brain regions by painful stimuli in migraine [66]. The decreased complexity of neurons in the insula and temporal pole cortex may impair their information integration function, leading to recurrent headache attacks and the manifestation of complex non-pain symptoms in migraine patients.

A significant reduction in NDI was observed in the right middle temporal and fusiform in CM. The temporal lobe plays a crucial role in multisensory integration, language processing, and regulation of emotions and memory [65–67]. Morphological analyses of migraines with and without aura reveal that both groups of migraine patients exhibit a significant reduction in temporal lobe gray matter volume (GMV) compared to HC [68]. The reduction of dendrites in the mid-temporal cortex may be due to a long-term, migraine-specific neurotoxic mechanism, and explains multisensory symptoms with CM. The fusiform gyrus is involved in both visual perception and processing of emotions [69]. The amplitude of low-frequency fluctuations (ALLF) in the right fusiform gyrus is reduced in migraineurs with comorbid depression. This reduction is negatively correlated with the severity of the headache [70]. Reduced neurites in right fusiform gyrus cortex in CM might be more likely to comorbid depression and exacerbate headache severity.

Both models suggested white and gray matter damage in migraineurs. It suggests that migraine may be a disorder characterized by disrupted white matter connectivity. The disrupted connections of various fiber tracts also implicated that the migraine was a heterogeneous disease. These cortical gray matter areas of the reduced neurites were correlated with pain processing, perception, and emotional regulation, shedding light on the pathological mechanisms of migraine, which are associated with cortical gray matter microstructural remodeling. These brain regions may become potential targets for neuromodulation therapy in migraine. The current research also showed a marked right lateralization of neurite loss, underlying mechanisms that warrant further investigation.

Existing studies have found that the cortical and subcortical neural circuits and networks associated with pain and chronic pain interact with the regulation of neurotransmitters [71]. Migraine is often considered a low serotonin syndrome. Reduced serotonin levels in

the brain lower the pain threshold, and tricyclic antidepressants also reduce the frequency of migraine attacks by increasing serotonin signaling, further supporting the role of serotonin in migraine pathology [72]. The increased SERT might lead to enhanced serotonin reuptake, reducing its concentration in the synaptic cleft. The genetic studies have highlighted the relationship of SERT protein gene with migraine susceptibility. However, serotonergic biochemistry is complex, and it is clear that a combination of factors (rather than any single factor) contributes to the migraine phenotype [15]. Our finding suggests that following dendritic damage in cortical gray matter, the distribution density of SERT increases, leading to reduced serotonin levels, which may trigger the onset of migraine. Dopaminergic stimulation induces most of the symptoms of a migraine. Dopamine receptor hypersensitivity exists in migraine. Dopaminergic agonists induce yawning, nausea, vomiting, hypotension, and other symptoms of migraine attacks at doses that do not impact individuals without migraine. While on the contrary, dopamine receptor antagonists were effective medications for the treatment of migraine [73]. A research based on an inflammatory soup-induced CM animal model suggests that activation of the D2 inhibits CM-related pain sensitization by blocking the GluA2/ROS positive feedback loop both in vivo and in vitro, indicating that the D2 may be a potential therapeutic target for CM [74]. The studies of PET have reported a significant decrease in presynaptic FDOPA in the right putamen of patients with chronic pain [75]. There is limited research on FDOPA concerning migraine. The results of both previous studies and this research suggest that dopaminergic system dysfunction may be a significant pathological mechanism in migraine, particularly highlighting the dopamine D2 receptor as a potential target with development value for migraine pharmacological treatment.

The disruption of neurotransmitter balance might lead to adaptive changes in neuronal microstructure in the cortical gray matter. Restoring neurotransmitter equilibrium might reduce neurobiological alterations associated with migraine. These alterations included the reduction of cortical gray matter and the damage of neuronal structure. Therefore, maintaining or restoring the homeostasis of neurotransmitters may represent a novel approach for migraine management.

Limitations and future directions

Certain limitations are present in this research. The cross-sectional design of the study cannot draw causal conclusions. Future longitudinal studies are needed to delve the deeper into this enigma. Although this study identified abnormalities of neurites in WM and cortical GM, further validation is required. The validation should be conducted in multicenter and large cohort research. The lack of histopathological evidence for these results warrants cautious interpretation. Due to restriction of imaging equipment and algorithms, the neural circuits in the cortex and subcortex require further investigation. Due to the absence of tissue-specific masks for other brain regions (white matter, brainstem, and subcortical nuclei), this study was limited to a preliminary exploration of the association between cortical gray matter microstructural alterations and neurotransmitter distributions. Additionally, there is a vast space to explore relationship between neurotransmitters and changes in neuronal microstructure. We acknowledge that we overlooked the menstrual status of female participants when scheduling the MRI scans. In future studies, we will ensure that menstrual cycle-related hormonal changes are carefully documented. Despite the limitations of our study, the results remain important and contribute new insights into the field of migraine research.

Conclusion

Across several brain regions, neurites are diminished in both migraine and CM. As the migraine progresses into chronicity, the axonal damage may become more pronounced. These findings indicated that neurite damage may be a pathological feature of migraine. The loss of cortical gray matter neurites is negatively associated with neurotransmitters. The present research reveals the central mechanisms underlying migraine onset and chronicity and offers potential targets for novel drug development and neuromodulation therapy.

Abbreviations

DTI	Diffusion Tensor Imaging
NODDI	Neurite Orientation Dispersion and Density Imaging
EM	Episodic Migraine
CM	Chronic Migraine
HCs	Healthy Controls
MA	Migraine with Aura
MO	Migraine without Aura
NDI	Neuronal Density Index
ODI	Orientation Dispersion Index
ISOVF	Isotropic Volume Fraction
FA	Fractional Anisotropy
MD	Mean Diffusivity
AD	Axial Diffusivity
RD	Radial Diffusivity
TBSS	Tract-Based Spatial Statistics
SBA	Surface-Based Analysis
BBR	Boundary-Based Registration
CSD	Cortical Spreading Depression
CSF	Cerebrospinal Fluid
SERT	Serotonin Transporter
DAT	Dopamine Transporter
FDOPA	6-Fluoro-(18 F)-L-3,4-Dihydroxyphenylalanine
GABAa	Gamma-Aminobutyric Acid Type A
MU	μ-Opioid Receptors
VAChT	Vesicular Acetylcholine Transporter
mGluR5	Metabotropic Glutamate Receptor 5
CB1	Cannabinoid 1 Receptor
NMDA	N-Methyl-D-Aspartic Acid Receptor
KappaOp	Kappa Opioid Receptor
NAT	Noradrenaline Transporter

GLM	Generalized Linear Model
TFCE	Threshold-Free Cluster Enhancement
FEW	Family-Wise Error
SLF	Superior Longitudinal Fasciculus
ILF	Inferior Longitudinal Fasciculus
UF	Uncinate Fasciculus
IFOF	Inferior Fronto-Occipital Fasciculus
CGH	Cingulum (Hippocampus)
BCC	Corpus Callosum
CST	Corticospinal Tract
ATR	Anterior Thalamic Radiation
WM	White Matter
GM	Gray Matter
BMI	Body Mass Index
VAS	Visual Analog Scale
HIT-6	Headache Impact Test-6
PHQ-9	Patient Health Questionnaire-9
GAD-7	Generalized Anxiety Disorder-7
PSQI	Pittsburgh Sleep Quality Index
MoCA	Montreal Cognitive Assessment

Supplementary Information

The online version contains supplementary material available at https://doi.org/10.1186/s10194-025-02059-3.

Supplementary Material 1

Acknowledgements
This work was supported by a team at the Tiantan Neuroimaging Center of the China National Clinical Research Center for Neurological Diseases.

Author contributions
ZLL conceived the study, with XYY, YGW, and BBS offering guidance throughout the process. ZLL and YLM analyzed the clinical and MRI data to confirm the findings. All authors were involved in data collection and discussions. ZLL wrote the initial draft of the manuscript, and all authors provided feedback on the revised version and approved the final manuscript.

Funding
The National Natural Science Foundation of China (grant numbers 32170752, 91849104, and 31770800), the Joint Funds of the National Natural Science Foundation of China (grant numbers U24A20683) and the National Natural Science Foundation of Beijing (grant number Z200024) supported this research.

Data availability
Data can be made available upon request.

Declarations

Ethics approval and consent to participate
Complete information about the study was shared with all participants. Afterward, they voluntarily provided their signature on the informed consent form. Study was registered with ClinicalTrials.gov (NCT05334927) and obtained ethical approval from Beijing Tiantan Hospital, Capital Medical University (no. KY2022-044).

Consent for publication
All authors authorize the publication.

Competing interests
The authors declare no competing interests.

Author details
[1]Department of Neurology, The Second Hospital of Lanzhou University, Cuiying Gate, No. 82 Linxia Road, Chengguan District, Lanzhou 730000, China
[2]Headache Center, Department of Neurology, Beijing Tiantan Hospital, Capital Medical University, No.119 South Fourth Ring West Road, Fengtai District, Beijing 100070, China
[3]Tiantan Neuroimaging Center of Excellence, China National Clinical Research Center for Neurological Diseases, Beijing Tiantan Hospital, Capital Medical University, No.119 South Fourth Ring West Road, Fengtai District, Beijing 100070, China

Received: 12 March 2025 / Accepted: 1 May 2025
Published online: 14 May 2025

References

1. Ashina M, Katsarava Z, Do TP et al (2021) Migraine: epidemiology and systems of care [J]. Lancet 397(10283):1485–1495
2. Steiner TJ, Stovner LJ (2023) Global epidemiology of migraine and its implications for public health and health policy [J]. Nat Rev Neurol 19(2):109–117
3. Dodick DW (2018) Migraine [J]. Lancet 391(10127):1315–1330
4. Hagen Stovnerlj, Linde K (2022) The global prevalence of headache: an update, with analysis of the influences of methodological factors on prevalence estimates [J]. J Headache Pain 23(1):34
5. Headache Classification Committee of the International Headache Society (IHS) (2018) 38(1): 1-211
6. Schwedt TJ, Chiang CC, Chong CD et al (2015) Functional MRI of migraine [J]. Lancet Neurol 14(1):81–91
7. Kuner R, Flor H (2016) structural plasticity and reorganisation in chronic pain [J]. Nat Rev Neurosci 18(1):20–30
8. Bertels Z, Singh H, Dripps I et al (2021) neuronal complexity is attenuated in preclinical models of migraine and restored by HDAC6 Inhibition [J]. Elife, 10
9. Planchuelo-gómez Á, García-azorín D, Guerrero Á L et al (2020) Gray matter structural alterations in chronic and episodic migraine: A morphometric magnetic resonance imaging study [J]. Pain Med 21(11):2997–3011
10. Rahimi R, Dolatshahi M, Abbasi-feijani F et al (2022) Microstructural white matter alterations associated with migraine headaches: a systematic review of diffusion tensor imaging studies [J]. Brain Imaging Behav 16(5):2375–2401
11. Shibata Y (2024) neurite damage in patients with migraine [J]. Neurol Int 16(2):299–311
12. Zhao L, Zhao W, Cao J et al (2023) Causal relationships between migraine and microstructural white matter: a Mendelian randomization study [J]. J Headache Pain 24(1):10
13. Zhang H, Schneider T, Wheeler-kingshott CA et al (2012) NODDI: practical in vivo neurite orientation dispersion and density imaging of the human brain [J]. NeuroImage 61(4):1000–1016
14. Xie YF, Huo FQ, Tang JS (2009) cerebral cortex modulation of pain [J]. Acta Pharmacol Sin 30(1):31–41
15. Gasparini CF, Smith RA, Griffiths LR (2017) Genetic and biochemical changes of the serotonergic system in migraine pathobiology [J]. J Headache Pain 18(1):20
16. Kim DJ, Jassar H, Lim M et al (2021) Dopaminergic regulation of reward system connectivity underpins pain and emotional suffering in migraine [J]. J Pain Res 14:631–643
17. O'hare L, Asher tarasil (2023) j m, excitation-Inhibition imbalance in migraine: from neurotransmitters to brain oscillations [J]. Int J Mol Sci, 24(12)
18. Dukart J, Holiga S, Rullmann M et al (2021) juspace: a tool for Spatial correlation analyses of magnetic resonance imaging data with nuclear imaging derived neurotransmitter maps [J]. Hum Brain Mapp 42(3):555–566
19. Dai W, Qiu E, Lin X et al (2023) Abnormal Thalamo-Cortical interactions in overlapping communities of migraine: an edge functional connectivity study [J]. Ann Neurol 94(6):1168–1181
20. Mori S, Zhang J (2006) Principles of diffusion tensor imaging and its applications to basic neuroscience research [J]. Neuron 51(5):527–539
21. Toniolo S (2022) What plasma biomarkers tell Us about hippocampal microstructural changes in Alzheimer's disease [J]. Brain 145(6):1880–1882
22. Fukutomi H, Glasser MF, Murata K et al (2019) diffusion tensor model links to neurite orientation dispersion and density imaging at high b-value in cerebral cortical Gray matter [J]. Sci Rep 9(1):12246
23. Timmers I, Roebroeck A, Bastiani M et al (2016) Assessing microstructural substrates of white matter abnormalities: A comparative study using DTI and NODDI [J]. PLoS ONE 11(12):e0167884

24. Nazeri A, Schifani C, Anderson JAE et al (2020) In vivo imaging of Gray matter microstructure in major psychiatric disorders: opportunities for clinical translation [J]. Biol Psychiatry Cogn Neurosci Neuroimaging 5(9):855–864
25. Kamiya K, Hori M (2020) noddi in clinical research [J]. J Neurosci Methods 346:108908
26. Sepehrband F, Clark KA, Ullmann JF et al (2015) Brain tissue compartment density estimated using diffusion-weighted MRI yields tissue parameters consistent with histology [J]. Hum Brain Mapp 36(9):3687–3702
27. Grussu F, Schneider T, Tur C et al (2017) Neurite dispersion: a new marker of multiple sclerosis spinal cord pathology? [J]. Ann Clin Transl Neurol 4(9):663–679
28. Seyedmirzaei H, Nabizadeh F, Aarabi MH et al (2023) neurite orientation dispersion and density imaging in multiple sclerosis: A systematic review [J]. J Magn Reson Imaging 58(4):1011–1029
29. Howes OD, Cummings C, Chapman GE et al (2023) Neuroimaging in schizophrenia: an overview of findings and their implications for synaptic changes [J]. Neuropsychopharmacology 48(1):151–167
30. Smith SM Jenkinsonm, Johansen-berg H et al (2006) tract-based Spatial statistics: Voxelwise analysis of multi-subject diffusion data [J]. NeuroImage 31(4):1487–1505
31. Brodoehl S, Gaser C, Dahnke R et al (2020) surface-based analysis increases the specificity of cortical activation patterns and connectivity results [J]. Sci Rep 10(1):5737
32. Zhang S, She S, Qiu Y et al (2023) altered cortical myelin in the salience and default mode networks in major depressive disorder patients: A surface-based analysis [J]. J Affect Disord 340:113–119
33. Zhang S, Wang Y, Zheng S et al (2022) multimodal mri reveals alterations of the anterior Insula and posterior cingulate cortex in bipolar II disorders: A surface-based approach [J]. Prog Neuropsychopharmacol Biol Psychiatry 116:110533
34. Villemonteix T, Guerreri M, Deantoni M et al (2023) sleep-dependent structural neuroplasticity after a Spatial navigation task: A diffusion imaging study [J]. J Neurosci Res 101(7):1031–1043
35. Premi E, Dukart J, Mattioli I et al (2023) Unravelling neurotransmitters impairment in primary progressive aphasias [J]. Hum Brain Mapp 44(6):2245–2253
36. Ren J, Yan L, Zhou H et al (2023) unraveling neurotransmitter changes in de Novo GBA-related and idiopathic Parkinson's disease [J]. Neurobiol Dis 185:106254
37. Planchuelo-gómez Á, García-azorín D, Guerrero Á L et al (2020) White matter changes in chronic and episodic migraine: a diffusion tensor imaging study [J]. J Headache Pain 21(1):1
38. Chou BC, Lerner A, Barisano G et al (2023) Functional MRI and diffusion tensor imaging in migraine: A review of migraine functional and white matter microstructural changes [J]. J Cent Nerv Syst Dis 15:11795735231205413
39. Christensen RH, Ashina H, Al-khazali H, M et al (2024) differences in cortical morphology in people with and without migraine: A registry for migraine (REFORM) MRI study [J]. Neurology 102(9):e209305
40. Zhang X, Zhou J, Guo M et al (2023) a systematic review and meta-analysis of voxel-based morphometric studies of migraine [J]. J Neurol 270(1):152–170
41. Zhang J, Wu YL, Su J et al (2017) assessment of Gray and white matter structural alterations in migraineurs without aura [J]. J Headache Pain 18(1):74
42. Barrio-arranz G, De luis-garcía R, Tristán-vega A et al (2015) Impact of MR acquisition parameters on DTI scalar indexes: A tractography based approach [J]. PLoS ONE 10(10):e0137905
43. Yu D, Yuan K, ZHAO L et al (2013) White matter integrity affected by depressive symptoms in migraine without aura: a tract-based Spatial statistics study [J]. NMR Biomed 26(9):1103–1112
44. Yu D, Yuan K, Qin W et al (2013) Axonal loss of white matter in migraine without aura: a tract-based Spatial statistics study [J]. Cephalalgia 33(1):34–42
45. Coppola G, Di Renzo A, Tinelli E et al (2020) patients with chronic migraine without history of medication overuse are characterized by a peculiar white matter fiber bundle profile [J]. J Headache Pain 21(1):92
46. Herbet G, Zemmoura I (2018) functional anatomy of the inferior longitudinal fasciculus: from historical reports to current hypotheses [J]. Front Neuroanat 12:77
47. Parlatini V, Radua J, Dell'acqua F et al (2017) Functional segregation and integration within fronto-parietal networks [J]. NeuroImage 146:367–375
48. Li X, Rangelov D Mattingleyjb et al (2023) White matter microstructure is associated with the precision of visual working memory [J]. NeuroImage 272:120069
49. Cole J, Chaddock CA, Farmer AE et al (2012) White matter abnormalities and illness severity in major depressive disorder [J]. Br J Psychiatry 201(1):33–39
50. Rayhan RU, Stevens BW, Timbol CR et al (2013) Increased brain white matter axial diffusivity associated with fatigue, pain and hyperalgesia in Gulf war illness [J]. PLoS ONE 8(3):e58493
51. Von Der Heide RJ, Skipper LM Klobusickye et al (2013) Dissecting the uncinate fasciculus: disorders, controversies and a hypothesis [J]. Brain 136(Pt 6):1692–1707
52. Fabri M (2013) Polonara G. functional topography of human corpus callosum: an FMRI mapping study [J]. Neural Plast, 2013: 251308
53. Horton JE, Crawford HJ, Harrington G et al (2004) Increased anterior corpus callosum size associated positively with hypnotizability and the ability to control pain [J]. Brain 127(Pt 8):1741–1747
54. Vogt BA (2005) Pain and emotion interactions in subregions of the cingulate gyrus [J]. Nat Rev Neurosci 6(7):533–544
55. Erpelding N, Davis KD (2013) Neural underpinnings of behavioural strategies that prioritize either cognitive task performance or pain [J]. Pain 154(10):2060–2071
56. Chong CD, Schwedt TJ (2015) Migraine affects white-matter tract integrity: A diffusion-tensor imaging study [J]. Cephalalgia 35(13):1162–1171
57. Tracey I, Mantyh PW (2007) The cerebral signature for pain perception and its modulation [J]. Neuron 55(3):377–391
58. Mainero C, Boshyan J (2011) Altered functional magnetic resonance imaging resting-state connectivity in periaqueductal Gray networks in migraine [J]. Ann Neurol 70(5):838–845
59. Li Z, Mei Y, Wang W et al (2024) White matter and cortical Gray matter microstructural abnormalities in new daily persistent headache: a NODDI study [J]. J Headache Pain 25(1):110
60. Burke MJ, Joutsa J, Cohen AL et al (2020) Mapping migraine to a common brain network [J]. Brain 143(2):541–553
61. Chen C, Yan M, Yu Y et al (2019) Alterations in regional homogeneity assessed by fMRI in patients with migraine without aura [J]. J Med Syst 43(9):298
62. Mammadkhanli O, Kehaya S (2024) Insular cortex involvement in migraine patients with chronic pain: A volumetric radiological and clinical study [J]. J Clin Neurosci 123:157–161
63. Borsook D, Veggeberg R, Erpelding N et al (2016) The Insula: A hub of activity in migraine [J]. Neuroscientist 22(6):632–652
64. Olson IR Plotzkera (2007) The enigmatic Temporal pole: a review of findings on social and emotional processing [J]. Brain 130(Pt 7):1718–1731
65. Schwedt TJ (2013) Multisensory integration in migraine [J]. Curr Opin Neurol 26(3):248–253
66. Moulton EA, Becerra L, Maleki N et al (2011) Painful heat reveals hyperexcitability of the Temporal pole in interictal and ictal migraine States [J]. Cereb Cortex 21(2):435–448
67. Zachlod D, Kedo O (2022) Anatomy of the Temporal lobe: from macro to micro [J]. Handb Clin Neurol 187:17–51
68. Bonanno L, Lo Buono V, De Salvo S et al (2020) Brain morphologic abnormalities in migraine patients: an observational study [J]. J Headache Pain 21(1):39
69. Barkhof F, Haller S, Rombouts SA (2014) Resting-state functional MR imaging: a new window to the brain [J]. Radiology 272(1):29–49
70. Ma M, Zhang J, Chen N et al (2018) Exploration of intrinsic brain activity in migraine with and without comorbid depression [J]. J Headache Pain 19(1):48
71. Kuner R (2021) Cellular circuits in the brain and their modulation in acute and chronic pain [J]. Physiol Rev 101(1):213–258
72. Jackson JL, Shimeall W (2010) Tricyclic antidepressants and headaches: systematic review and meta-analysis [J]. BMJ 341:c5222
73. Peroutka SJ (1997) Dopamine and migraine [J]. Neurology 49(3):650–656
74. Zhang W, Zhang X (2024) LEI M, Dopamine D2 receptor activation blocks GluA2/ROS positive feedback loop to alienate Chronic-Migraine-Associated pain sensitization [J]. Antioxid (Basel), 13(6)
75. JääSkelälnen SK, Rinne JO Forssellh et al (2001) Role of the dopaminergic system in chronic pain -- a fluorodopa-PET study [J]. Pain 90(3):257–260

Publisher's note